Journal of Hazardous Materials 211–212 (2012) 208–217

Contents lists available at ScienceDirect

Journal of Hazardous Materials

journal homepage: www.elsevier.com/locate/jhazmat

Catalytic hydrodechlorination of chloroaromatic gas streams promoted by Pd and Ni: The role of hydrogen spillover

Claudia Amorim[a], Mark A. Keane[b,*]

[a] Department of Chemical and Materials Engineering, University of Kentucky, Lexington, KY, USA
[b] Chemical Engineering, School of Engineering and Physical Sciences, Heriot-Watt University, Edinburgh EH14 4AS, Scotland, United Kingdom

ARTICLE INFO

Article history:
Received 1 June 2011
Received in revised form 2 August 2011
Accepted 7 August 2011
Available online 12 August 2011

Keywords:
Hydrodechlorination
Spillover hydrogen
Chlorobenzene
1,3-Dichlorobenzene
Bulk Pd and Ni catalysts
Al_2O_3 supported nano-scale Pd and Ni

ABSTRACT

Catalytic hydrodechlorination (HDC) is an effective means of detoxifying chlorinated waste. Involvement of spillover hydrogen is examined in gas phase dechlorination of chlorobenzene (CB) and 1,3-dichlorobenzene (1,3-DCB) over Pd and Ni. The catalytic action of single component Pd and Ni, Pd/Al_2O_3, Ni/Al_2O_3 and physical mixtures with Al_2O_3 has been considered. Catalyst activation is characterized in terms of temperature programmed reduction, the supported nano-scale metal phase by transmission electron microscopy and hydrogen/surface interactions by chemisorption/temperature programmed desorption. Pd/Al_2O_3 generated significantly greater amounts of spillover hydrogen (by a factor of over 40) compared with Ni/Al_2O_3. Hydrogen spillover on Pd/Al_2O_3 far exceeded the chemisorbed component, whereas chemisorbed and spillover content was equivalent for Ni/Al_2O_3. Inclusion of Al_2O_3 with Ni and Ni/Al_2O_3 increased spillover with an associated increase in specific HDC rate (up to a factor of 10) and enhanced selectivity to benzene from 1,3-DCB. HDC rate delivered by Pd and Pd/Al_2O_3 was largely unaffected by the addition of Al_2O_3. This can be attributed to the higher intrinsic HDC performance of Pd that results in appreciable HDC activity under conditions where Ni/Al_2O_3 was inactive. Spillover was partially recovered (post TPD) for the Ni samples but the loss was irreversible in the case of Pd.

1. Introduction

Chlorine containing effluent discharge has a direct adverse impact on stratospheric ozone, ecosystems and public health. There is now a pressing need for a robust chloro-waste detoxification unit operation where the energy requirements must be weighed against the possibility of recycle. The standard control strategies involve some form of "end-of-pipe" treatment, notably incineration and catalytic/chemical oxidation. Complete combustion of chloroarenes, the subject of this study, requires elevated temperatures (>1200 K) and excess oxygen [1], where products of incomplete combustion (e.g. polychlorodibenzodioxins (PCDD) and polychlorodibenzofurans (PCDF)) exhibit high toxicity [2]. Catalytic combustion has lower energy demands and reduced NOx emissions [3] but can still generate significant quantities of PCCD/PCDF, with CO_2 release and products such as CO, Cl_2 and $COCl_2$ that are difficult to trap [4]. In any case, the irreversible loss of raw material that results from combustion runs counter to the progressive concept of low waste technologies. Application of photolysis, ozonation and supercritical oxidation represent advanced oxidation technologies but the efficiency of each is unproven and all are hampered by high energy demands [5–7]. Catalytic hydrodechlorination (HDC), hydrogen cleavage of C–Cl bonds, represents an alternative approach that lowers toxicity and generates reusable raw material [8,9]. A move from incineration to HDC results in immediate savings in terms of fuel and/or chemical recovery. Kalnes and James [10], in a pilot-scale study clearly showed the economic advantages of HDC over incineration where the energy required to run the HDC process in terms of generating the hydrogen consumed can be subtracted from the energy in the recycled fuel product to give a net energy production. The catalytic HDC unit can be incorporated in distillation/separation lines with HCl recovery by absorption into an aqueous phase to produce a dilute acid solution that can be concentrated downstream. The HCl effluent can be further trapped in basic solution, the hydrogen gas scrubbed and washed to remove trace contaminants and recycled to the reactor [11]. Moreover, Brinkman et al. [12] have demonstrated the feasibility of a full scale hydrotreatment of PCB (polychlorinated biphenyl) contaminated lubricating oils by catalytic HDC. However, a loss of activity with time on-stream has been a feature of gas phase HDC and ascribed to coke deposition and/or the formation of surface metal halides and/or metal sintering [13].

While thermal (non-catalytic) HDC requires temperatures in excess of 773 K [14,15], catalytic HDC operates under much lower, even sub-ambient [16], temperatures due to the ability of the catalytic metal phase to dissociate molecular hydrogen, generating

* Corresponding author. Tel.: +44 0 131 4514719.
E-mail address: M.A.Keane@hw.ac.uk (M.A. Keane).

0304-3894/$ – see front matter © 2011 Elsevier B.V. All rights reserved.
doi:10.1016/j.jhazmat.2011.08.025

reactive H atoms that facilitate C–Cl scission [17]. It follows that an enhanced supply of H atoms should improve overall HDC performance. Anchoring a catalytically active metal to a carrier allows control over metal particle size at the nano-scale with, ideally, a commensurate increase in catalyst efficiency. Although typical oxide supports (e.g. Al_2O_3, SiO_2, MgO and zeolites) do not, in the absence of a metal phase, promote HDC under mild conditions [18–20], possible synergistic effects such as the occurrence of hydrogen spillover may have a role to play. Spillover hydrogen, i.e. the migration of atomic hydrogen to the catalyst support after H_2 dissociation on the metallic surface, has been the subject of a diverse literature [21,22]. Hydrogen spillover has been demonstrated for metals that are known to dissociatively adsorb H_2 (Pd [21,24–26], Ni [27–29], Pt [19,26,29], Rh [18,30], Ru [31,32]) when supported on carbon [18,21,23–25,32], Al_2O_3 [18,19,29,32], SiO_2 [27,28,30], TiO_2 [32], zeolite [18], WO_3 [26] and MoO_3 [28]. Of direct relevance to this study, Kramer and Andre [29] demonstrated the occurrence of hydrogen spillover on Pt/Al_2O_3 and Ni/Al_2O_3 but not on the Al_2O_3 support alone. However, hydrogen incorporation on metal-free Al_2O_3 was observed after treatment with H atoms generated by high-frequency discharge. These results indicate that Al_2O_3 can accommodate H atoms, formed either as the result of spillover from a supported metal phase or externally generated and supplied from the gas phase.

The participation of spillover hydrogen in hydrogenation [18–20,33,34] and hydrogenolysis [20,35–39] reactions has been reported in the literature. Moreover, there is some evidence for a contribution in the HDC of chlorobenzene over Ni/SiO_2 [20,28,40], Ni_2P/SiO_2 [41,42], Pd/Al_2O_3 [35,39] and Pd/C [43] and the HDC of 1,2,4-trichlorobenzene over Ni/Nb_2O_5 [44]. A kinetic analysis of gas phase HDC over supported Ni has addressed surface reaction dynamics and the involvement of spillover hydrogen in determining HDC rate [28,39,45]. One approach to probing spillover effects is to employ physical (or mechanical) mixtures of the support with bulk metals and directly compare the resultant catalytic response with that delivered by the catalytic metal without support addition. The use of such physical mixtures (supported Rh, Pt and Ni mixed with Al_2O_3, SiO_2, carbon, MgO, zeolite and WO_3/Al_2O_3) has been explored to some extent in hydrogenation reactions [18–20,33]. Similar studies [20,40] applied to HDC are limited to reaction over Ni catalysts with SiO_2 addition but have not been coupled with any characterization analysis. In this report, we link critical characterization measurements to catalytic HDC data. We consider the action of bulk and Al_2O_3 supported Pd and Ni and physical mixtures with Al_2O_3. Pd and Ni were adopted as the catalytic agents since group VIII noble metals are known to be effective in HDC reactions [13,46,47]. Chlorobenzene and 1,3-dichlorobenzene served as model reactants and are representative of high priority pollutants generated in the manufacture of dyes and a diversity of agrochemicals [13].

2. Experimental

2.1. Catalyst preparation and activation

The γ-Al_2O_3 support (Puralox) was supplied by Condea Vista Co. and used as received. Pd/Al_2O_3 (5.4%, w/w) and Ni/Al_2O_3 (4.8%, w/w) were prepared by standard impregnation where 2-butanolic $Pd(NO_3)_2$ or $Ni(NO_3)_2$ solutions were added at 353 K to the Al_2O_3 substrate with constant agitation (500 rpm), oven dried at 393 K for 16 h and sieved (ATM fine test sieves) into batches of 75 μm average particle diameter. The metal loading was determined by inductively coupled plasma-optical emission spectrometry (ICP-OES, Vista-PRO, Varian Inc.). Bulk PdO (99.998%) and bulk NiO (99%), the sources of unsupported Pd and Ni, respectively, were obtained from Sigma–Aldrich. Physical mixtures of Al_2O_3 with PdO and NiO were also employed (metal content = 5%, w/w) to facilitate direct comparison with the impregnated catalysts. Prior to reaction, the catalyst precursors were activated in a 60 $cm^3\ min^{-1}$ stream of ultra-pure H_2 at 10 K min^{-1} to 523 ± 1 K (Pd) and 723 ± 1 K (Ni), which was maintained for 1–12 h. The activated samples were passivated at room temperature in a stream of 1% (v/v) O_2/He (mass flow controlled at 20 $cm^3\ min^{-1}$) for *ex situ* analysis.

2.2. Catalyst characterization

BET surface area, temperature programmed reduction (TPR), H_2 chemisorption and temperature programmed desorption (TPD) analyses were conducted using the commercial CHEMBET 3000 (Quantachrome Instrument) unit, equipped with a thermal conductivity detector (TCD). A known mass (≤0.5 g) of sample was loaded into a U-shaped Pyrex glass cell (10 cm × 3.76 mm i.d.) and BET surface areas were recorded with a 30% (v/v) N_2/He flow where pure N_2 (99.9%) served as the internal standard. At least 2 cycles of N_2 adsorption–desorption in the flow mode were employed to determine total surface area by the standard single point method with data acquisition/manipulation using the TPR Win™ software. Temperature programmed reduction was conducted in 5% (v/v) H_2/N_2 (mass flow controlled at 20 $cm^3\ min^{-1}$) at a heating rate of 10 K min^{-1} to 523 K (Pd) or 723 K (Ni), where the effluent gas was directed through a liquid N_2 trap. The reduced samples were swept with a flow of N_2 for 1 h, cooled to room temperature and subjected to H_2 chemisorption using a pulse (50 μl) titration procedure. At this pulse volume, the maximum partial pressure of H_2 in the sample cell (0.004 atm) was well below 0.013 atm, the pressure needed for Pd hydride formation at room temperature [48,49]. Hydrogen pulse introduction was repeated until the signal area was constant, indicating surface saturation. The samples were then thoroughly flushed with N_2 for 30 min to remove physisorbed H_2 and TPD was conducted in N_2 at 50 K min^{-1} to 873 K. Based on TCD calibration and analysis of the effluent gas using a MICROMASS PC Residual Gas Analyser, the TPD profiles recorded in this paper can be attributed solely to H_2 release. After TPD, an additional TPR/H_2 chemisorption/TPD sequence was conducted. Samples of 7.8% (w/w) Pd/activated carbon and 8.5% (w/w) Ni/activated carbon were also subjected to the same analysis. Preparation and characterization details for the carbon supported metals have been reported previously [50]. BET surface area and H_2 chemisorption values were reproducible to within ±3% and the values quoted in this paper are the mean. Powder X-ray diffractograms (Philips X'Pert unit using Ni filtered Cu Kα radiation) were consistent with a cubic symmetry for bulk Pd and Ni: peaks at 40.1°, 46.7°, 68.1° and 82.15° corresponding to (1 1 1), (2 0 0), (2 2 0) and (3 1 1) Pd planes; peaks at 44.5°, 51.8° and 76.3°, corresponding to (1 1 1), (2 0 0) and (2 2 0) Ni planes [51]. Transmission electron microscopy (TEM) analyses of alumina supported Pd and Ni were conducted using a JEOL 2000 TEM microscope operated at an accelerating voltage of 200 kV. The catalyst sample was dispersed in 1-butanol by ultrasonic vibration, deposited on a lacey-carbon/Cu grid (200 Mesh) and dried at 383 K for 12 h before TEM analysis.

2.3. Catalysis procedure

Reactions were carried out in the gas phase under atmospheric pressure in a fixed bed glass reactor (i.d. = 15 mm) with a co-current flow of chlorobenzene (CB) or 1,3-dichlorobenzene (1,3-DCB) in H_2. The catalytic reactor, and operating conditions to ensure negligible heat/mass transport limitations, have been described in detail elsewhere [52,53] but some features, pertinent to this study, are given below. In order to control the contact time, glass powder (sieved in the same mesh range as the catalyst) was used as bed

Table 1
Reaction conditions employed for CB and 1,3-DCB HDC hydrogenation over Pd and Ni catalysts.

Metal	Catalyst	Catalyst composition	Reactant	Reduction conditions	Reaction temperature (K)	Cl/metal ($mol_{Cl}\ mol_{metal}^{-1}\ h^{-1}$)	Contact time (s)
Pd	Pd	–[a]	CB	523 K/1 h	423	289	0.1
	$Pd + Al_2O_3$	5% (w/w) Pd					
	Pd/Al_2O_3	–[a]				3062	0.2
	$Pd/Al_2O_3 + Al_2O_3$	1:2[b]					
		1:10[b]					
		1:20[b]					
Ni	Ni	–[a]	CB	723 K/12 h	573	4	1.4
			1,3-DCB				
	$Ni + Al_2O_3$	5% (w/w) Ni	CB			4	1.4
			1,3-DCB				
	Ni/Al_2O_3	–[a]	CB			90	1.4
			1,3-DCB				
	$Ni/Al_2O_3 + Al_2O_3$	1:2[b]	CB			90	1.4
		1:10[b]	CB				
			1,3-DCB				
		1:20[b]	CB			90	1.4

[a] Single component bed (no Al_2O_3 diluent).
[b] Catalyst:Al_2O_3 weight ratio.

diluent. The reaction conditions employed in this study are given in Table 1. In the case of bulk and supported Ni systems, reactions were conducted pre- and post-TPD. The chloroarene reactant was fed by means of a microprocessor controlled infusion pump (Model 100, kd Scientific) *via* a glass/teflon air tight syringe and teflon line to the reactor in a stream of ultra pure H_2, the flow rate of which was monitored using a Humonics 520 digital flow meter. A layer of glass beads served as a preheating zone to ensure that the reactant was vaporised and reached the reaction temperature before contacting the catalyst bed. The reactor effluent was collected in a liquid nitrogen trap for subsequent analysis, which was conducted using a PerkinElmer Auto System XL chromatograph equipped with a split/splitless injector and a flame ionization detector, employing a DB-1 50 m × 0.20 mm i.d., 0.33 μm capillary column (J&W Scientific). The relative peak area % was converted to mol% using detailed calibrations where the detection limit typically corresponded to a feedstock conversion <0.4 mol%: overall analytic reproducibility was better than ±3%. Repeated catalytic runs with different samples from the same batch of catalyst delivered product compositions that were reproducible to within ±5%. The degree of hydrodechlorination (x_{Cl}) is given by

$$x_{Cl} = \frac{[HCl]_{out}}{[Cl_{org}]_{in}}$$

where $[Cl_{org}]$ ($mol\ dm^{-3}$) represents Cl concentration associated with the aromatic feed; *in* and *out* refer to the inlet and outlet reactor streams, respectively. It has been demonstrated elsewhere [54] that HCl is the sole inorganic product with no Cl_2 detected in the product stream. Fractional 1,3-DCB conversion (x_{DCB}) is given by

$$x_{DCB} = \frac{[DCB]_{in} - [DCB]_{out}}{[DCB]_{in}}$$

Table 2
BET surface area associated with the activated bulk metals (with/without Al_2O_3 addition) and alumina supported Pd and Ni and the volume of H_2 chemisorbed pre- and post-TPD (per gram of catalyst).

Sample	BET surface area ($m^2\ g^{-1}$)	H_2 uptake ($cm^3\ g^{-1}$)	
		pre-TPD	Post-TPD
Pd	2	0.3	0.2
$Pd + Al_2O_3$	178	0.5	0.4
Pd/Al_2O_3	143	5.6	5.4
Ni	1	0.1	0.1
$Ni + Al_2O_3$	180	0.1	0.1
Ni/Al_2O_3	134	7.2	6.9
Al_2O_3	190	–	–

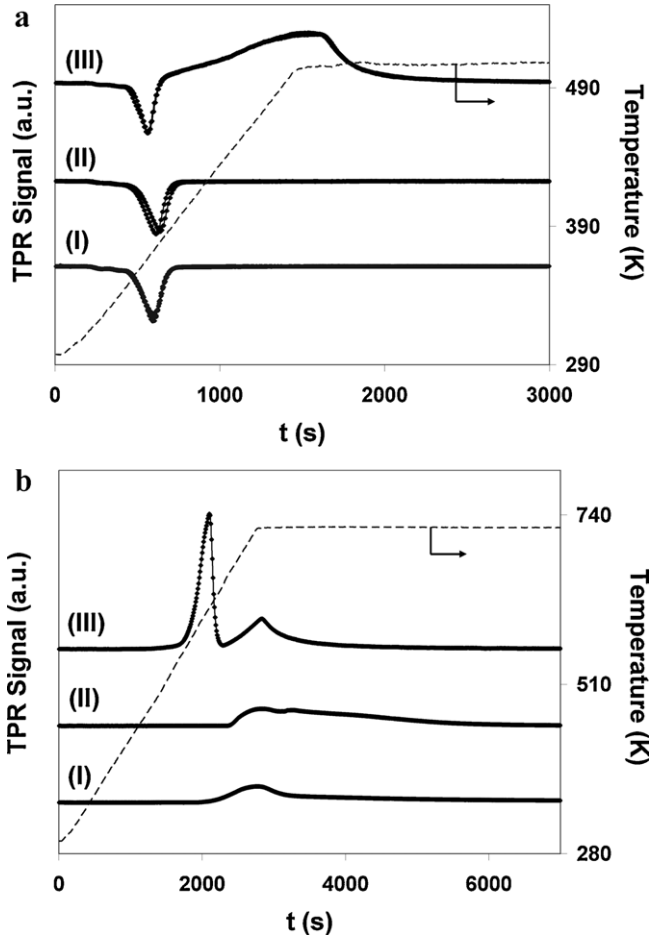

Fig. 1. TPR profiles: (a) PdO (I), $PdO + Al_2O_3$ (II) and Pd/Al_2O_3 (III); (b) NiO (I), $NiO + Al_2O_3$ (II) and Ni/Al_2O_3 (III).

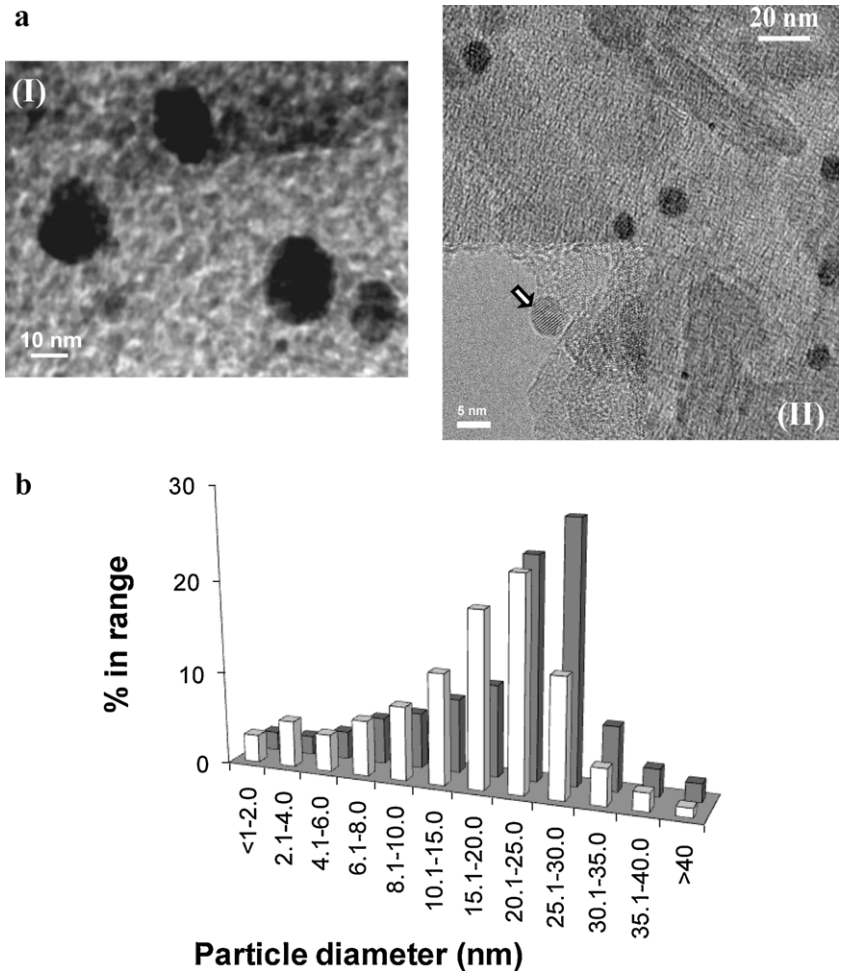

Fig. 2. (a) Representative TEM images of (I) Ni/Al_2O_3 and (II) Pd/Al_2O_3 with (b) Ni/Al_2O_3 (solid bars) and Pd/Al_2O_3 (open bars) particle size distribution histograms. Note: Isolated Pd particle in the higher magnification image is indicated by the arrow.

and the selectivity (%) with which benzene ($S_{benzene}$) was produced from DCB is calculated from

$$S_{benzene}(\%) = \frac{[benzene]_{out}}{[DCB]_{in} - [DCB]_{out}} \times 100$$

The CB (99.9%) and 1,3-DCB (98%) reactants (Sigma–Aldrich) were used without further purification; ultra pure (99.999%) H_2, He and N_2 was supplied by Scott-Gross Co. Inc.

3. Results and discussion

3.1. Catalyst characterization: BET, TPR and TEM

The BET surface areas of the activated catalysts considered in this study given in Table 2. The lower areas recorded for Pd/Al_2O_3 and Ni/Al_2O_3 compared with the Al_2O_3 support can be attributed to partial pore blockage by the impregnated metal phase. The temperature programmed reduction profiles generated for the catalyst precursors (bulk metal oxide, physical mixtures and alumina supported metals) are given in Fig. 1(a) and (b) for Pd and Ni systems, respectively. The level of reproducibility of the TPR profiles can be assessed from the repeated measurements included in Fig. 1. The TPR profiles recorded for bulk PdO, in the presence or absence of physically mixed Al_2O_3, are characterized by a single negative peak (H_2 production) at 381 ± 3 K. This can be attributed to H_2 release resulting from the decomposition of Pd hydride, which is formed by H_2 absorption where the partial pressure exceeds 0.013 atm [55,56]. The absence of a positive TPR peak (H_2 consumption) in advance of hydride decomposition suggests reduction to zero valent Pd prior to the temperature ramp. Indeed, a room temperature reduction of supported [57,58] and unsupported PdO [59] has been reported elsewhere. The temperature corresponding to maximum H_2 release/hydride decomposition for bulk Pd is higher than that (368 K, Profile III) recorded for Pd/Al_2O_3. The decomposition of supported Pd hydride has been reported to occur over the temperature range 323–373 K [58–62] and is shifted to higher values with an increase in H_2 partial pressure [63] and Pd particle size [56]. The latter is consistent with our observation that a higher temperature was required for bulk Pd hydride decomposition relative to the Al_2O_3 supported system. In addition to H_2 release/hydride decomposition, TPR of Pd/Al_2O_3 also generated a broad positive peak during the temperature ramp that extended into the final isothermal hold (523 K). This response suggests support interaction that serves to stabilize the Pd precursor, requiring elevated temperatures for reduction. This is in line with previous reports wherein H_2 consumption peaks up to 523 K were recorded for the TPR of PdO supported on Al_2O_3 [64,65].

In contrast to the Pd system, the TPR profiles (Fig. 1(b)) generated for the Ni samples presented only positive peaks with H_2 consumption during the temperature ramp and final isotherm hold (723 K). The T_{max} corresponding to the first and second peak in the TPR profile of Ni/Al_2O_3 is 628 K and 723 K, respectively, where the latter peak is common to the unsupported systems. The TPR profile for NiO (with and without Al_2O_3 addition) yielded a broad peak that

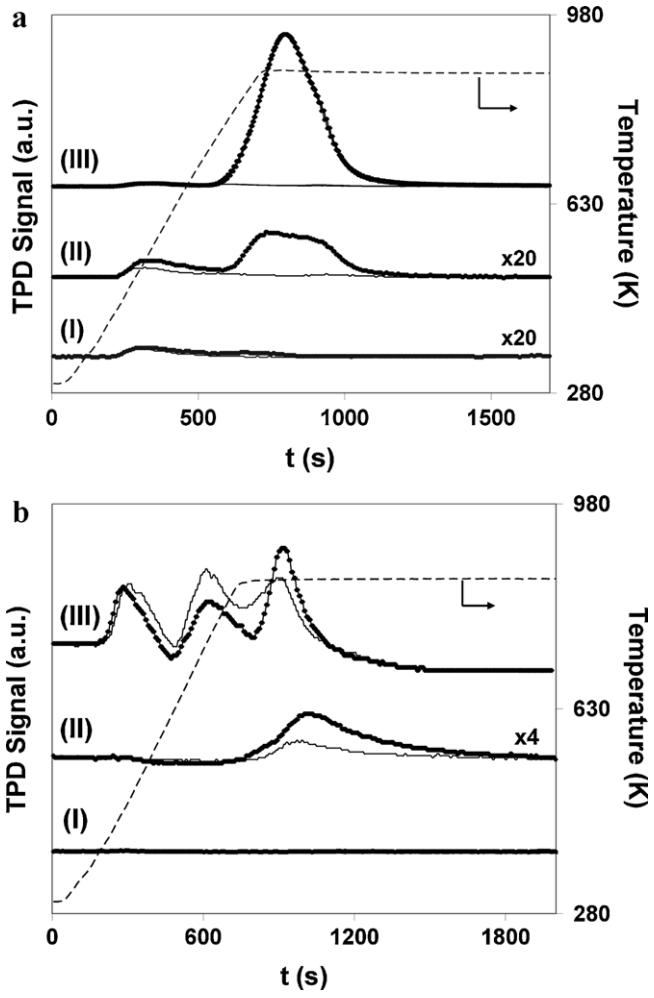

Fig. 3. Hydrogen TPD profiles: (a) Pd (I), Pd + Al_2O_3 (II) and Pd/Al_2O_3 (III); (b) Ni (I), Ni + Al_2O_3 (II) and Ni/Al_2O_3 (III); first (♦) and second (solid line) TPD.

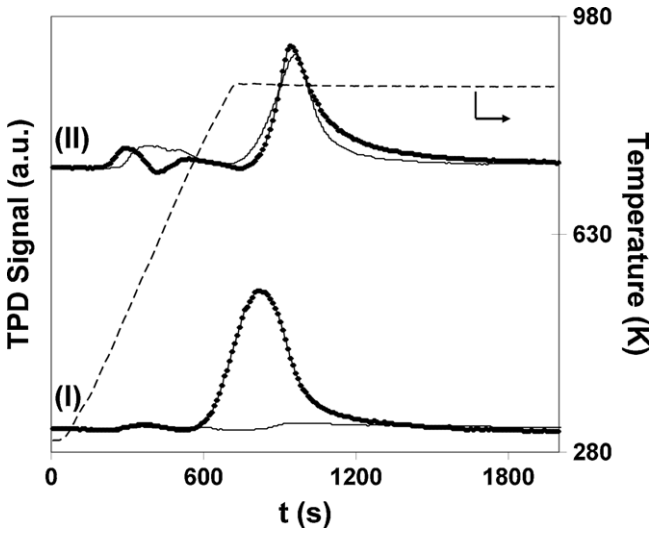

Fig. 4. Hydrogen TPD profiles for Pd/AC (I) and Ni/AC (II): first (♦) and second (solid line) TPD.

extended into the isothermal region and is consistent with earlier reports [66,67]. A two stage reduction has been proposed [40,68] for the TPR of supported nickel nitrate where thermal decomposition to NiO precedes the subsequent reduction of NiO to Ni^0 and can account for the two TPR peaks recorded in Fig. 1(b). The presence of one [66,69], two [68,70] and even four [67] reduction peaks in TPR profiles of Ni/Al_2O_3 has been reported. The TPR response is influenced by metal/support interactions which, in turn, are sensitive to catalyst preparation, metal loading and pretreatment [69]. The TEM images provided in Fig. 2(a) serve to illustrate the nature of the metal dispersion in the activated catalysts where the supported particles exhibit a pseudo-spherical morphology. The Pd and Ni particle size distribution histograms presented in Fig. 2(b) are based on total metal particle counts in excess of 800. Both supported systems are characterized by a distribution of nano-scale particles where the majority (>90% of total count) have diameters <30 nm.

3.2. Catalyst characterization: H_2 chemisorption-TPD

Hydrogen chemisorption values, pre- and post-TPD, are given in Table 2. The role of Al_2O_3 in dispersing the Pd or Ni phase is immediately apparent from the higher (by over an order of magnitude) H_2 uptake on Pd/Al_2O_3 and Ni/Al_2O_3 compared with the respective bulk metals. Based on H_2 chemisorption, unsupported Pd and Ni particle size is in the 10^{-6}–10^{-7} m range. Hydrogen TPD generated the profiles presented in Fig. 3. The TPD profile for bulk Pd exhibited an ill defined desorption peak at *ca.* 570 K. The volume of H_2 released matched (to within 5%) that taken up in the chemisorption step (see Table 2). The absence of any H_2 release at $T < 400$ K due to Pd hydride decomposition (observed for TPR (see Fig. 1(a)) is consistent with an exclusive H_2 chemisorption during pulse titration. The Pd + Al_2O_3 physical mixture and Pd/Al_2O_3 delivered a TPD response that is quite distinct in that two H_2 desorption peaks were observed. The lower temperature peak (T_{max} = 520–560 K) represents release of the chemisorbed H_2 component, i.e. H_2 release from Pd. The additional high temperature peak, which extends into the final isothermal hold, was only generated in the presence of Al_2O_3, either as an additive in the physical mixture or as support, which is consistent with the involvement of hydrogen spillover on Al_2O_3. Hydrogen TPD from bulk Ni did not result in a measurable signal (Fig. 3(b)), i.e. H_2 release was below detection limits (<0.02 cm^3 H_2 g^{-1}). The TPD profile generated for Ni/Al_2O_3 presents three stages of H_2 desorption with respective T_{max} values of 483, 785 and 873 K. The Ni + Al_2O_3 physical mixture exhibited a single broad TPD peak that coincides with the highest temperature peak of Ni/Al_2O_3, a response that matches that observed for Pd. In the case of Ni/Al_2O_3, the amount of H_2 adsorbed corresponds to the total desorption associated with the two lower temperature peaks. The appearance of three H_2 desorption peaks from Ni/Al_2O_3 (T_{max} = *ca.* 410, 720 and 820 K) has also been reported by Cesteros et al. [71], who linked the high temperature desorption to hydrogen spillover. In a series of blank runs, we did not observe any H_2 consumption or release by/from the Al_2O_3 support alone over the same temperature range. This was expected and is consistent with the available literature [18,30,72,73]. However, the capability of Al_2O_3 to accommodate spillover hydrogen has been demonstrated and associated with surface acidity [18]. Hydrogen spillover species have been viewed as electron donors where an acidic surface (as electron acceptor) enhances electron transfer and facilitates transport from the metal site [22]. Indeed, Sermon and Bond [74] have noted a correlation between concentration of spillover hydrogen and the number of hydroxyl groups associated with the support.

Hydrogen TPD is a practical approach to studying spillover effects for supported metals as it allows some differentiation between hydrogen associated with the metal and the support. There are a number of published H_2 TPD profiles where desorption from the metal phase and from the support is seen to occur at different temperatures [18,23,29,32]. Taking an overview of the literature, desorption of spillover hydrogen is characterized by

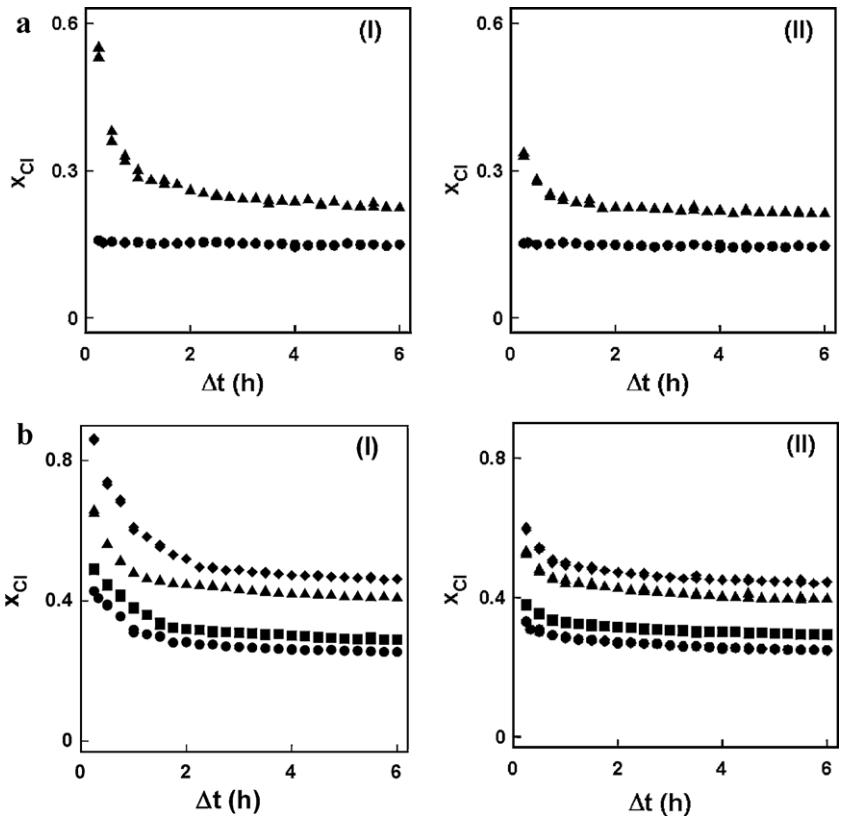

Fig. 5. Fractional CB HDC (x_{Cl}) as a function of time-on-stream over: (a) Ni (●) and Ni + Al_2O_3 (▲); (b) Ni/Al_2O_3 (●), Ni/Al_2O_3 + Al_2O_3 (1:2, w/w ratio) (■), Ni/Al_2O_3 + Al_2O_3 (1:10, w/w ratio) (▲) and Ni/Al_2O_3 + Al_2O_3 (1:20, w/w ratio) (♦); reaction pre-(I) and post-(II) TPD. Note: Repeated runs are included to illustrate experimental reproducibility.

a TPD response at $T > 503$ K regardless of the metal or support [18,23,27–29,32,72]. Ouchaib et al. [23] reported two H_2 desorption peaks from charcoal supported Pd at 373 K and 673 K, attributing the higher temperature peak to spillover hydrogen. Benseradj et al. [18], by applying H_2 TPD analysis to characterize Rh/Al_2O_3 physically mixed with Al_2O_3, SiO_2, activated carbon and zeolite, noted that the desorption peak due to spillover hydrogen (T_{max} in the range 503–873 K) increased with incremental additions of support to Rh/Al_2O_3. Kramer and Andre [29] observed an additional high temperature TPD peak (*ca.* 753 K) for Pt/Al_2O_3 that was not present in the profile for unsupported Pt. Such observations agree with the TPD behaviour recorded in this study. The occurrence of hydrogen spillover in catalyst + support physical combinations where the two components are well mixed [18,31,75] or are present as discrete layers [31] has been demonstrated with a reported [31,76] spillover transport across non-contiguous surfaces. At the same Pd content in the physical mixture (Pd + Al_2O_3) and Pd/Al_2O_3, the amount of hydrogen spillover was an order of magnitude higher for the latter, i.e. 560 cm^3 H_2 g^{-1} compared with 53 cm^3 H_2 g^{-1}. In the case of Ni, spillover release from Ni/Al_2O_3 (13 cm^3 H_2 g^{-1}) was four times greater than that recorded for Ni + Al_2O_3 (3 cm^3 H_2 g^{-1}). The increased amount of spillover associated with the supported metals must result from a greater degree of contact where the metal/interface is extended.

Furthermore, Pd generated appreciably greater amounts of spillover hydrogen (by a factor of over 40) compared with Ni. We can tentatively link this to the significantly higher diffusion coefficient for H_2 in Pd (*ca.* 10^{-11} m^2 s^{-1}) relative to Ni (*ca.* 10^{-14} m^2 s^{-1}) [77,78], i.e. more efficient transfer from metal to support. It should also be noted that while the extent of spillover hydrogen on Pd/Al_2O_3 was far greater than that chemisorbed on Pd, the chemisorbed and spillover component on Ni/Al_2O_3 was essentially equivalent. Faccin et al., in an FTIR study [79], reported evidence of hydrogen spillover on Pd/TiO_2 and not on Ni/TiO_2 but the authors did not provide any explicit explanation for this response. In order to ascertain whether the degree of spillover is determined by the metal phase alone, we applied the same TPR/H_2 chemisorption/TPD analysis to Pd/AC and Ni/AC. The resultant TPD profiles are presented in Fig. 4 where it can be seen that both samples delivered similar H_2 release at 873 K. Hydrogen desorption from Pd/Al_2O_3 was appreciably greater (seven-fold) than that recorded for Pd/AC while Ni/AC generated three times more spillover hydrogen than Ni/Al_2O_3. Differences in the amounts of spillover hydrogen associated with the same metal supported on different carriers [32,72] and different metals anchored to the same support [80] have been recorded in the literature. Spillover can be influenced by several factors such as the nature of the hydrogen donor (H_2, cyclohexene, NH_3, toluene), the concentration of initiating and acceptor sites, degree of contact between the participating phases, temperature, catalyst activation, temperature of hydrogen adsorption and metal-support interaction(s) [26,32,70,72]. Given the number of interrelated factors that can impact on the spillover response, it is difficult to decouple such contributions and explicitly assign one dominant factor. Our results demonstrate quite different behaviour for two metal/two carrier combinations where the metal phase or support alone does not appear to govern the degree of spillover and contributions due to the metal/support interface must be critical.

As spillover hydrogen was removed during TPD to 873 K, all the samples were subjected to a second sequence of TPR/H_2 chemisorption/TPD in order to check whether the initial level of spillover can be restored. The published review articles that have addressed hydrogen spillover phenomena have focused on the impact of spillover on catalytic reactions [31,81], the methods of spillover detection [74], the chemical nature of spillover species [22] and spillover mechanisms [31] but with no reference to spillover

Table 3
Initial CB and 1,3-DCB HDC rates, DCB fractional conversion (x_{DCB}) and selectivity with respect to benzene ($S_{benzene}$ (%)) over bulk and alumina supported Ni (with/without Al_2O_3 addition) for reaction pre- and post-TPD.

Reactant	Catalyst	Catalyst bed composition	HDC rate ($mol_{Cl}\ g_{Ni}^{-1}\ h^{-1}$)		$S_{benzene}$ (%)	x_{DCB}
			pre-TPD	post-TPD	pre-TPD	
CB	Ni	–[a]	10×10^{-3}	10×10^{-3}		
	$Ni + Al_2O_3$	5% (w/w) Ni	37×10^{-3}	22×10^{-3}		
	Ni/Al_2O_3	–[a]	62×10^{-2}	52×10^{-2}		
	$Ni/Al_2O_3 + Al_2O_3$	1:2[b]	72×10^{-2}	59×10^{-2}		
		1:10[b]	100×10^{-2}	80×10^{-2}		
		1:20[b]	132×10^{-2}	89×10^{-2}		
1,3-DCB	Ni	–[a]	4×10^{-3}	4×10^{-3}	46	0.08
	$Ni + Al_2O_3$	5% (w/w) Ni	37×10^{-3}	21×10^{-3}	74	0.72
	Ni/Al_2O_3	–[a]	19×10^{-2}	15×10^{-2}	54	0.17
	$Ni/Al_2O_3 + Al_2O_3$	1:10[b]	76×10^{-2}	44×10^{-2}	89	0.58

[a] Single component bed (no Al_2O_3 diluent).
[b] Catalyst:Al_2O_3 (w/w) ratio.

reversibility or regeneration. The levels of hydrogen chemisorption were largely retained (albeit detectably lower) after the first TPD, as can be seen from the entries in Table 2. The initial level of hydrogen spillover was restored to some degree in the case of the Ni samples (*ca.* 40% for $Ni + Al_2O_3$ and 70% for Ni/Al_2O_3) but there was no detectable higher temperature desorption from the Pd samples during the second TPD (Fig. 3(a)). A decrease in spillover hydrogen in the Ni system may result from a partial Ni sintering during the first TPD, as suggested by the lower H_2 uptake on Ni/Al_2O_3 post-TPD (Table 2). Our tests show that once spillover hydrogen is removed (thermally at 873 K) from $Pd + Al_2O_3$ and Pd/Al_2O_3, it cannot be regenerated in a subsequent TPR/H_2 chemisorption cycle, i.e. the loss is irreversible. Spillover regeneration on Pd/AC and Ni/AC showed the same response (Fig. 4), i.e. spillover hydrogen on Ni/AC was recovered after the first TPD but Pd/AC did not exhibit any measurable spillover release. It is worth flagging the work of Miller et al. [72] who reported reversibility in terms of surface chemisorbed H_2 but an irreversible loss of hydrogen spillover from Pt supported on zeolite or Al_2O_3 after a TPD to 973 K. They attributed this effect to an irreversible removal of surface hydroxyl groups in the first TPD, which rendered the surface ineffective for the accommodation of spillover species. Our results suggest that the (re-)generation of hydrogen spillover is critically linked to the specific metal-support interface.

3.3. Role of hydrogen spillover in HDC

The reaction conditions employed in this study are given in Table 1. In the light of the TPD measurements, the use of physical mixtures can facilitate an explicit assignment of spillover contributions to HDC performance. As blank tests, passage of CB or 1,3-DCB in a stream of H_2 through the empty reactor or over the Al_2O_3 support alone, i.e. in the absence of Pd or Ni, did not result in any detectable conversion (under the conditions given in Table 1). The variation of the fractional dechlorination (x_{Cl}) of CB with time-on-stream over Ni (two reaction cycles) and Pd (one reaction cycle) catalysts are shown in Figs. 5 and 6, respectively; initial HDC rates are given in Tables 3 and 4. The results of repeated reaction runs are included to illustrate the degree of raw data reproducibility. In the case of the Ni systems, conversion of CB generated benzene as the sole product whereas cyclohexane (selectivity < 4%) was also isolated in the product stream generated over Pd as a result of a subsequent benzene hydrogenation. There was no detectable chlorocyclohexane formation, indicating that hydrogenation of the aromatic ring without concomitant dechlorination was not promoted. The formation of chlorocyclohexane has been reported for supported Pd catalysts but with very low selectivities (<0.1%) [82]. A temporal decline in HDC activity was observed in agreement with previous reports where this was ascribed to a catalyst poisoning by the HCl product [34,45]. With respect to the Ni system, the activity of bulk Ni (Fig. 5(a)) and Ni/Al_2O_3 (Fig. 5(b)) was enhanced with the addition of Al_2O_3 in the physical mixtures. The inclusion of Al_2O_3 resulted in an up to fourfold increase in CB HDC rate (Table 3), which we take as confirmation of the participation of hydrogen

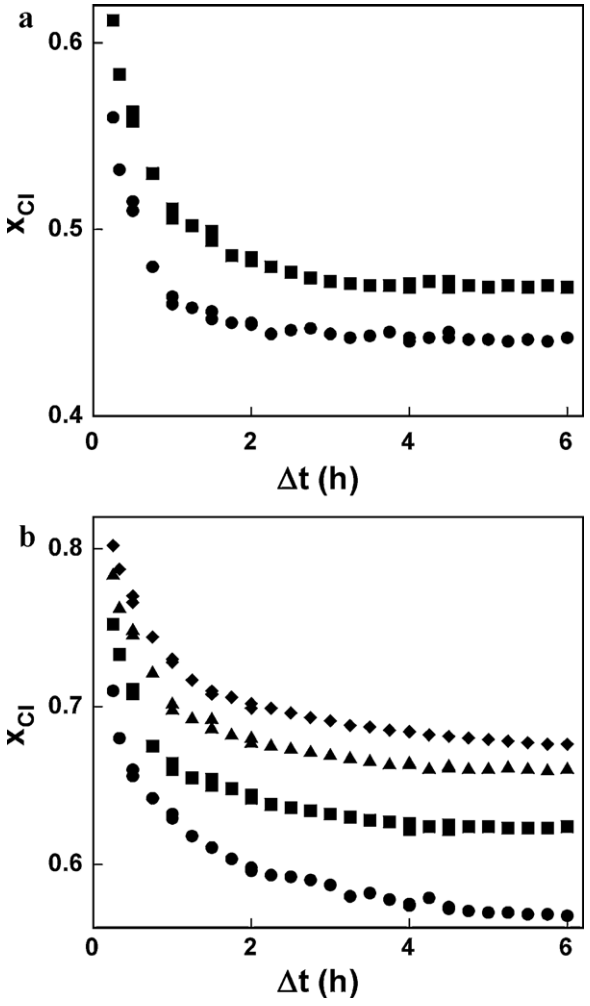

Fig. 6. Fractional CB HDC (x_{Cl}) as a function of time-on-stream over: (a) Pd (●) and $Pd + Al_2O_3$ (▲); (b) Pd/Al_2O_3 (●), $Pd/Al_2O_3 + Al_2O_3$ (1:2, w/w ratio) (■), $Pd/Al_2O_3 + Al_2O_3$ (1:10, w/w ratio) (▲) and $Pd/Al_2O_3 + Al_2O_3$ (1:20, w/w ratio) (♦). Note: Repeated runs are included to illustrate degree of experimental reproducibility.

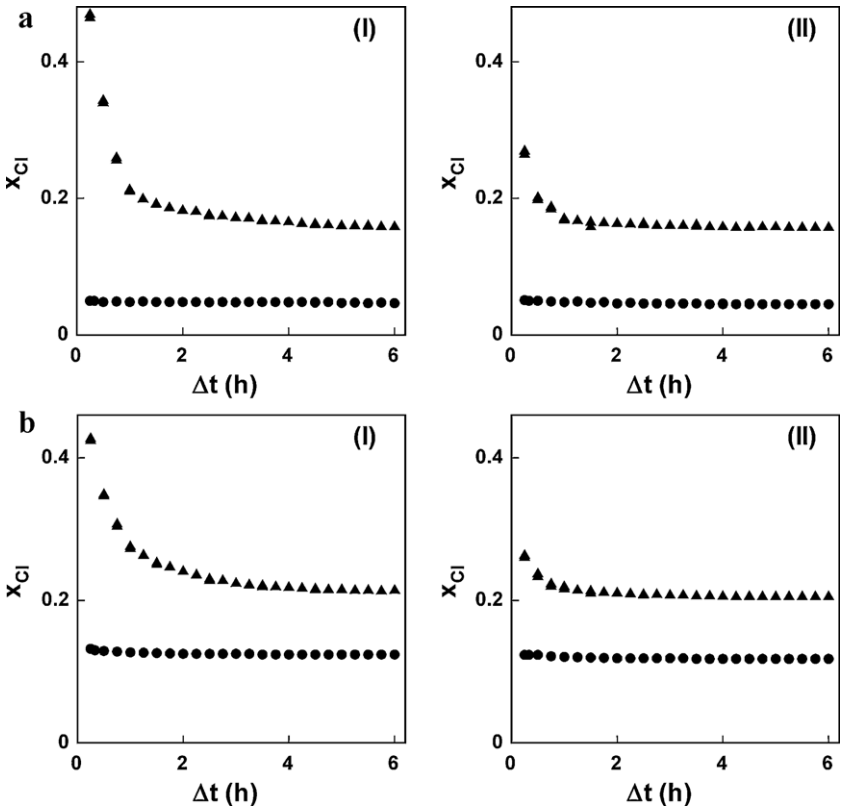

Fig. 7. Fractional 1,3-DCB HDC (x_{Cl}) as a function of time-on-stream over: (a) Ni (●) and Ni + Al_2O_3 (▲); (b) Ni/Al_2O_3 (●) and Ni/Al_2O_3 + Al_2O_3 (1:10, w/w ratio) (▲); reaction pre-(I) and post-(II) TPD. Note: Repeated runs are included to illustrate experimental reproducibility.

Table 4
Initial CB HDC rates delivered by bulk and alumina supported Pd (with and without Al_2O_3 addition).

Reactant	Catalyst	Catalyst bed composition	HDC rate ($mol_{Cl}\ g_{Pd}^{-1}\ h^{-1}$)
CB	Pd	–[a]	1.5
	Pd + Al_2O_3	5% (w/w) Pd	1.8
	Pd/Al_2O_3	–[a]	22.1
		1:2[b]	22.9
	Pd/Al_2O_3 + Al_2O_3	1:10[b]	24.8
		1:20[b]	25.2

[a] Single component bed (no Al_2O_3 diluent).
[b] Catalyst:Al_2O_3 (w/w) ratio.

spillover in HDC over Ni. While HDC rate increased with increasing Al_2O_3 content in the bed, this increase is not in direct proportion to the amount of Al_2O_3 added. Taking the observed enhancement in HDC rate to result from the contribution due to spillover hydrogen, the dependence of rate on Al_2O_3 content in the physical mixtures reflects the spillover content. The latter is governed by the degree of contact between Ni/Al_2O_3 and Al_2O_3 in the bed and the transport of hydrogen across the boundary between the physically mixed catalyst and support particles. Addition of Al_2O_3 also served to increase CB conversion over bulk and supported Pd (Fig. 6) but with a lesser enhancement of HDC rate (Table 4). It should be noted that the HDC rates (at 423 K) delivered by Pd were from 19 to 150 times greater than those measured (at 573 K) for Ni. Under the same reaction conditions, Ni/Al_2O_3 was inactive when Pd/Al_2O_3 delivered a fractional CB dechlorination (x_{Cl}) of 0.77. These results demonstrate that Pd is far more effective as a HDC agent than Ni, as has been noted elsewhere [35,40,83]. As a point of reference, Simagina et al. [83], studying the HDC of hexachlorobenzene, recorded a 95% conversion over Pd/C under reaction conditions where Ni/C did not exhibit any activity. The results suggest that Pd is intrinsically so active that hydrogen spillover contributions due the addition of Al_2O_3 are not significant under the stated reaction conditions.

As H_2 TPD analysis of the Ni catalysts revealed a capacity for spillover regeneration (see Fig. 3(b)), a second reaction cycle (post-TPD) was conducted to assess the catalytic consequences. The resultant temporal dependence of CB fractional conversion is shown in Fig. 5. The HDC rates delivered by bulk Ni were equivalent in both cycles whereas Ni/Al_2O_3 exhibited a detectable loss of activity post-TPD. The physical mixtures involving bulk Ni and Ni/Al_2O_3 again outperformed the catalysts without Al_2O_3 addition, albeit the initial HDC rate was lower relative to the first reaction cycle (Table 3) and a temporal decline in conversion was again in evidence (Fig. 5). The drop in HDC rate in the second cycle can be associated with the partial recovery of spillover hydrogen post-TPD (Fig. 3(b)). The role of spillover hydrogen in determining HDC was probed further by considering the HDC of 1,3-DCB over bulk Ni and Ni/Al_2O_3 with/without Al_2O_3 addition. The time-on-stream activity response is shown in Fig. 7, where two reaction cycles are again considered. Conversion of 1,3-DCB generated CB and benzene with, again, no detectable cyclohexane or chlorocyclohexane in the product stream. The generation of CB as product suggests a stepwise dechlorination and it has been demonstrated elsewhere [84] that sequential, as opposed to concerted dechlorination, predominates in the gas phase HDC of 1,3-DCB over supported Ni catalysts [84]. As in the case of CB HDC: (i) the addition of Al_2O_3 to supported or unsupported Ni resulted in an appreciable increase (by up to a factor of 10) in HDC rate (Table 3); (ii) the improvement in activity extended to the second reaction cycle where the lower HDC rate relative to that obtained pre-TPD can be ascribed to an incomplete restoration of the initial spillover complement. There is evidence in the literature [85–87] that gas phase chloroarene HDC over supported Ni catalysts proceeds *via* an electrophilic

mechanism involving an arenium ion intermediate and the presence of a second electron withdrawing Cl substituent on the ring destabilizes the rate determining transition complex with a resultant decrease in reactivity. Indeed, 1,3-DCB HDC rate over Ni and Ni/Al_2O_3 was lower than that of CB. It should, however, be noted that bulk Ni physically mixed with Al_2O_3 delivered equivalent CB and DCB HDC rates (see Table 3). This response illustrates the effectiveness of spillover hydrogen to promote HDC. Moreover, the benzene selectivities recorded in Table 3 clearly demonstrate that the inclusion of Al_2O_3 served to elevate appreciably the extent of complete HDC to benzene. Our work has explicitly demonstrated the participation of spillover hydrogen in hydrogenolytic C–Cl bond scission. In addition to the role of Al_2O_3 as a source of spillover hydrogen, we cannot discount a possible involvement arising from chloroarene activation *via* interaction with Al_2O_3. It has been reported in the literature that haloarenes can adsorb from the gas phase not only on the metal phase [40,82] but also on the Al_2O_3 support [88,89]. While flagging this as a possible contributing factor, we have limited this study to a consideration of the role of reactive hydrogen in determining HDC performance. Future work will focus on the nature of chloroarene/surface interactions (with both metal and support) leading to catalytic HDC.

4. Conclusion

A comparison of the catalytic action of Pd, Ni, Pd/Al_2O_3 and Ni/Al_2O_3 with and without the inclusion of Al_2O_3 (as physical mixtures) has facilitated an assessment of the role of spillover hydrogen in chloro-aromatic HDC. Hydrogen TPD from Al_2O_3 supported metal and bulk metal + Al_2O_3 mixtures exhibited an additional high temperature peak due to spillover desorption. Pd/Al_2O_3 generated significantly greater quantities (by a factor of over 40) of spillover hydrogen relative to Ni/Al_2O_3. Spillover from Pd/Al_2O_3 was far in excess of chemisorbed H_2, whereas the chemisorbed and spillover components were equivalent on Ni/Al_2O_3. Addition of Al_2O_3 to bulk Ni and Ni/Al_2O_3 resulted in an enhancement of CB and 1,3-DCB HDC rate by up to a factor of 10, demonstrating the contribution of spillover hydrogen; Al_2O_3 by itself was inactive. HDC of 1,3-DCB over Ni generated CB as a partially dechlorinated intermediate where inclusion of Al_2O_3 significantly elevated the extent of complete HDC to benzene. Pd catalysts exhibited intrinsically higher HDC activities, where Pd/Al_2O_3 promoted dechlorination under reaction conditions where Ni/Al_2O_3 was inactive. Thermal desorption of spillover hydrogen from the Ni system was not wholly irreversible in that a partial recovery (with an associated partial improvement of catalyst performance) was possible in a subsequent catalyst activation. In contrast, the spillover content was not recoverable in the case of the Pd system. This work has established the role of spillover hydrogen in catalytic HDC and is a feature that should be incorporated in any process scale-up and/or industrial implementation. One immediate benefit of increasing spillover hydrogen content is the ability to operate HDC with a dilute hydrogen inlet stream, which is an important consideration in developing an effective (low cost) process where issues of atom efficiency and recycle must be addressed.

Acknowledgement

This work was supported in part by the National Science Foundation through grant CTS-0218591.

References

[1] A. Converti, M. Zilli, D.M. De Faveri, G. Ferraiolo, Hydrogenolysis of organochlorinated pollutants—kinetics and thermodynamics, J. Hazard. Mater. 27 (1991) 127–135.
[2] T. Pollock, Dioxins and Furans: Questions and Answers, Academy of Natural Sciences, Philadelphia, PA, 1989.
[3] R. Delaigle, D.P. Debecker, F. Bertinchamps, E.M. Gaigneaux, Revisiting the behaviour of vanadia-based catalysts in the abatement of (chloro)-aromatic pollutants: towards an integrated understanding, Top. Catal. 52 (2009) 501–516.
[4] J.R. Hart, Verification of dioxin formation in a catalytic oxidizer, Chemosphere 72 (2008) 75–78.
[5] B.Z. Li, X.Y. Xu, L. Zhu, Ozonation of chloronitrobenzenes in aqueous solution: kinetics and mechanism, J. Chem. Technol. Biotechnol. 84 (2009) 167–175.
[6] J.M. Shen, Z.L. Chen, Z.Z. Xu, X.Y. Li, B.B. Xu, F. Qi, Kinetics and mechanism of degradation of *p*-chloronitrobenzene in water by ozonation, J. Hazard. Mater. 152 (2008) 1325–1331.
[7] D.D. Dionysiou, A.P. Khodadoust, A.M. Kern, M.T. Suidan, I. Baudin, J.-M. Laîné, Effect of ionic strength and hydrogen peroxide on the photocatalytic degradation of 4-chlorobenzoic acid in water, Appl. Catal. B: Environ. 24 (2000) 139–155.
[8] Y. Bo, Y. Gang, Reductive destruction of environmental pollutants by hydrogenation process, Prog. Chem. 21 (2009) 217–226.
[9] M.A. Keane, A review of catalytic approaches to waste minimisation: case study–liquid phase catalytic hydrodechlorination of chlorophenols, J. Chem. Technol. Biotechnol. 80 (2005) 1211–1222.
[10] T.N. Kalnes, R.B. James, Hydrogenation and recycle of organic waste streams, Environ. Prog. 7 (1988) 185–191.
[11] M.A. Keane, Treating difficult and toxic chlorinated waste, Environ. Bus. Mag. 70 (2001) 12–13.
[12] D.W. Brinkman, J.R. Dickson, D. Wilkinson, Full scale hydrotreatment of polychlorinated biphenyls in the presence of used lubricating oils, Environ. Sci. Technol. 29 (1995) 87–91.
[13] M.A. Keane, Supported transition metals for hydrodechlorination reactions, ChemCatChem 3 (2011) 800–821.
[14] J.A. Manion, P. Mulder, R. Louw, Gas phase hydrogenolysis of polychlorobiphenyls, Environ. Sci. Technol. 19 (1985) 280–282.
[15] R. Louw, J.W. Rothuizen, R.C.C. Wegman, Vapour phase chemistry of arenes 2. Thermolysis of chlorobenzene and reactions with aryl radicals and chlorine and hydrogen atoms at 500 °C, J. Chem. Soc. Perkin Trans. 2 (1973) 1635–1640.
[16] G. Yuan, M.A. Keane, Liquid phase hydrodechlorination of chlorophenols at 273 K, Catal. Commun. 4 (2003) 195–201.
[17] L.N. Zanaveskin, V.A. Aver'yanov, Y.A. Treger, Prospects for the development of methods for the processing of organohalogen waste. Characteristic features of the catalytic hydrogenolysis of halogen-containing compounds, Russ. Chem. Rev. 65 (1996) 617–624.
[18] F. Benseradj, F. Sadi, M. Chater, Hydrogen spillover studies on diluted Rh/Al_2O_3 catalyst, Appl. Catal. A: Gen. 228 (2002) 135–144.
[19] J. Wang, L. Huang, Q. Li, Influence of different diluents in Pt/Al_2O_3 catalyst on the hydrogenation of benzene, toluene and o-xylene, Appl. Catal. A: Gen. 175 (1998) 191–199.
[20] M.A. Keane, G. Tavoularis, The role of spillover hydrogen in gas phase catalytic aromatic hydrodehalogenation and hydrogenation over nickel/silica, React. Kinet. Catal. Lett. 78 (2003) 11–18.
[21] A.L.D. Ramos, D.A.G. Aranda, M. Schmal, Hydrogen spillover measured by mass spectrometry during reduction of carbon supported palladium catalysts: effect of carbon properties, Stud. Surf. Sci. Catal. 138 (2001) 291–298.
[22] U. Roland, T. Braunschweig, F. Roessner, On the nature of spilt-over hydrogen, J. Mol. Catal. A: Chem. 127 (1997) 61–84.
[23] T. Ouchaib, B. Moraweck, J. Massardier, A. Renouprez, Charcoal supported palladium and palladium chromium catalysts: a comparison of the hydrogenation of dienes with silica supported metals, Catal. Today 7 (1990) 191–198.
[24] D.J. Suh, T.J. Park, S.K. Ihm, Effect of surface oxygen groups on carbon supports on the characteristics of Pd/C catalysts, Carbon 31 (1993) 427–435.
[25] Z.X. Cheng, S.B. Yuan, J.W. Fan, Q.M. Zhu, M.S. Zhen, Hydrogen spillover within carbon supported palladium catalysts prepared under ultrasound, Stud. Surf. Sci. Catal. 112 (1997) 261–266.
[26] P.A. Sermon, G.C. Bond, Studies of hydrogen spillover, J. Chem. Soc. Faraday Trans. I 76 (1980) 889–900.
[27] E.-J. Shin, M.A. Keane, Gas phase hydrogenation/hydrogenolysis of phenol over supported nickel catalysts, Ind. Eng. Chem. Res. 39 (2000) 883–892.
[28] E.-J. Shin, A. Spiller, G. Tavoularis, M.A. Keane, Chlorine-nickel interactions in gas phase hydrodechlorination: catalyst deactivation and the nature of reactive hydrogen, Phys. Chem. Chem. Phys. 1 (1999) 3173–3181.
[29] R. Kramer, M. Andre, Adsorption of atomic hydrogen on alumina by hydrogen spillover, J. Catal. 58 (1979) 287–295.
[30] M. Ojeda, M.L. Granados, S. Rojas, P. Terreros, J.L.G. Fierro, Influence of residual chloride ions in the CO hydrogenation over Rh/SiO_2 catalysts, J. Mol. Catal. A: Chem. 202 (2003) 179–186.
[31] W.C. Conner, J.L. Falconer, Spillover in heterogeneous catalysis, Chem. Rev. 95 (1995) 759–788.
[32] H.-Y. Lin, Y.-W. Chen, The kinetics of H_2 adsorption on supported ruthenium catalysts, Thermochim. Acta 419 (2004) 283–290.
[33] S.T. Srinivas, P.K. Rao, Direct observation of hydrogen spillover on carbon-supported platinum and its influence on the hydrogenation of benzene, J. Catal. 148 (1994) 470–477.

[34] H.L. Chen, H. Yang, O. Omotoso, L.H. Ding, Y. Briker, Y. Zheng, Z. Ring, Contribution of hydrogen spillover to the hydrogenation of naphthalene over diluted Pt/RHO catalysts, Appl. Catal. A: Gen. 358 (2009) 103–109.
[35] Y. Hashimoto, A. Ayame, Low-temperature hydrodechlorination of chlorobenzenes on platinum-supported alumina catalysts, Appl. Catal. A: Gen. 250 (2003) 247–254.
[36] L.M. Gomez-Sainero, A. Cortes, X.L. Seoane, A. Arcoya, Hydrodechlorination of carbon tetrachloride to chloroform in the liquid phase with metal-supported catalysts. Effect of the catalyst components, Ind. Eng. Chem. Res. 39 (2000) 2849–2854.
[37] V.S. Ranade, R. Prins, Hydrogenolysis of benzylic alcohols on rhodium catalysts, Chem. Eur. J. 6 (2000) 313–320.
[38] F. Valdevenito, R. Garcia, N. Escalona, F.J. Gil-Llambias, S.B. Rasmussen, A. Lopez-Agudo, Ni//Mo synergism via hydrogen spillover, in pyridine hydrodenitrogenation, Catal. Commun. 11 (2010) 1154–1156.
[39] Y. Hashimoto, Y. Uemichi, A. Ayame, Low-temperature hydrodechlorination mechanism of chlorobenzenes over platinum-supported and palladium-supported alumina catalysts, Appl. Catal. A: Gen. 287 (2005) 89–97.
[40] K.V. Murthy, P.M. Patterson, M.A. Keane, C–X bond reactivity in the catalytic hydrodehalogenation of haloarenes over unsupported and silica supported Ni, J. Mol. Catal. A: Chem. 225 (2005) 149–160.
[41] J.X. Chen, L.M. Sun, R.J. Wang, J.Y. Zhang, Hydrodechlorination of chlorobenzene over Ni_2P/SiO_2 catalysts: influence of Ni_2P loading, Catal. Lett. 133 (2009) 346–353.
[42] N.S. Babu, N. Lingaiah, J.V. Kumar, P.S.S. Prasad, Studies on alumina supported Pd-Fe bimetallic catalysts prepared by deposition-precipitation method for hydrodechlorination of chlorobenzene, Appl. Catal. A: Gen. 367 (2009) 70–76.
[43] C. Amorim, M.A. Keane, Palladium supported on structured and nonstructured carbon: a consideration of Pd particle size and the nature of reactive hydrogen, J. Colloid Interface Sci. 322 (2008) 196–208.
[44] K.V.R. Chary, K.S. Lakshmi, P.V.R. Rao, K.S.R. Rao, M. Papadaki, Characterization and catalytic properties of niobia supported nickel catalysts in the hydrodechlorination of 1,2,4-trichlorobenzene, J. Mol. Catal. A: Chem. 223 (2004) 353–361.
[45] M.A. Keane, D.Y. Murzin, A kinetic treatment of the gas phase hydrodechlorination of chlorobenzene over nickel/silica: beyond conventional kinetics, Chem. Eng. Sci. 56 (2001) 3185–3195.
[46] F.J. Urbano, J.M. Marinas, Hydrogenolysis of organohalogen compounds over palladium supported catalysts, J. Mol. Catal. A: Chem. 173 (2001) 329–345.
[47] M.A. Keane, Hydrodehalogenation of haloarenes over silica supported Pd and Ni—a consideration of catalytic activity/selectivity and haloarene reactivity, Appl. Catal. A: Gen. 271 (2004) 109–118.
[48] J.E. Benson, H.S. Hwang, M. Boudart, Hydrogen-oxygen titration method for the measurement of supported palladium surface areas, J. Catal. 30 (1973) 146–153.
[49] W. Palczewska, Catalytic reactivity of hydrogen on palladium and nickel hydride, Adv. Catal. 24 (1975) 245–291.
[50] C. Amorim, G. Yuan, P.M. Patterson, M.A. Keane, Catalytic hydrodechlorination over Pd supported on amorphous and structured carbon, J. Catal. 234 (2005) 268–281.
[51] JCPDS–ICDD, PCPDFWIN, Version 2.2, June 2001.
[52] G. Tavoularis, M.A. Keane, Gas phase catalytic dehydrochlorination and hydrodechlorination of aliphatic and aromatic systems, J. Mol. Catal. A: Chem. 142 (1999) 187–199.
[53] M.A. Keane, F. Cardenas-Lizana, S. Gomez-Quero, W. Shen, Alumina supported Ni-Au: surface synergistic effects in catalytic hydrodechlorination, ChemCatChem 1 (2009) 270–278.
[54] G. Tavoularis, M.A. Keane, Gas phase catalytic hydrodechlorination of chlorobenzene over nickel/silica, J. Chem. Technol. Biotechnol. 74 (1999) 60–70.
[55] L.L. Jewell, B.H. Davis, Review of absorption and adsorption in the hydrogen–palladium system, Appl. Catal. A: Gen. 310 (2006) 1–15.
[56] S. Gomez-Quero, F. Cardenas-Lizana, M.A. Keane, Effect of metal dispersion on the liquid phase hydrodechlorination of 2,4-dichlorophenol over Pd/Al_2O_3, Ind. Eng. Chem. Res. 47 (2008) 6841–6853.
[57] C.B. Wang, H.K. Lin, C.M. Ho, Effects of the addition of titania on the thermal characteristics of alumina-supported palladium, J. Mol. Catal. A: Chem. 180 (2002) 285–291.
[58] G.M. Tonetto, D.E. Damiani, Performance of Pd-Mo/gamma-Al_2O_3 catalysts for the selective reduction of NO by methane, J. Mol. Catal. A: Chem. 202 (2003) 289–303.
[59] C.-W. Chou, S.-J. Chu, H.-J. Chiang, C.-Y. Huang, C.-J. Lee, S.-R. Sheen, T.P. Perng, C.-T. Yeh, Temperature programmed reduction study on calcination of nano-palladium, J. Phys. Chem. B 105 (2001) 9113–9117.
[60] S.C. Shekar, J.K. Murthy, P.K. Rao, K.S.R. Rao, Pd supported on fluorinated carbon covered alumina (FCCA) a high performance catalyst in the hydrodechlorination of dichlorodifluoromethane, Catal. Commun. 4 (2003) 39–44.
[61] F. Pinna, M. Signoretto, G. Strukel, S. Polizzi, N. Pernicone, Pd-SiO_2 catalysts. Stability of β-PdH_x as a function of Pd dispersion, React. Kinet. Catal. Lett. 60 (1997) 9–13.
[62] M. Bonarowska, J. Pielaszek, W. Juszczyk, Z. Karpinski, Characterization of Pd-Au/SiO_2 catalysts by X-ray diffraction, temperature programmed hydride decomposition and catalytic probes, J. Catal. 195 (2000) 304–315.
[63] E.J.A.X. van de Sandt, A. Wiersma, M. Makkee, H. van Bekkum, J.A. Moulijn, Palladium black as model catalyst in the hydrogenolysis of CCl_2F_2 (CFC-12) into CH_2F_2 (HFC-32), Appl. Catal. A: Gen. 155 (1997) 59–73.
[64] G. Garcia, J.R. Vargas, M.A. Valenzuela, M. Rebollar, D. Acosta, Palladium supported on alumina catalysts prepared by MOCVD and impregnation methods, Mater. Res. Soc. Symp. 549 (1999) 237–242.
[65] F. Pinna, F. Menegazzo, M. Signoretto, P. Canton, G. Fagherazzi, N. Pernicone, Consecutive hydrogenation of benzaldehyde over Pd catalysts—influence of supports and sulfur poisoning, Appl. Catal. A: Gen. 219 (2001) 195–200.
[66] H.-S. Roh, K.-W. Jun, W.-S. Dong, J.-S. Chang, S.-E. Park, Y.-I. Joe, Highly active and stable Ni/Ce-ZrO_2 catalyst for H_2 production from methane, J. Mol. Catal. A: Chem. 181 (2002) 137–142.
[67] C.-W. Hu, J. Yao, H.-Q. Yang, Y. Chen, A.-M. Tian, On the inhomogeneity of low nickel loading methanation catalyst, J. Catal. 166 (1997) 1–7.
[68] C. Louis, Z.X. Cheng, M. Che, Characterization of Ni/SiO_2 catalyst during impregnation and further thermal activation treatment leading to metal particles, J. Phys. Chem. 97 (1993) 5703–5712.
[69] O. Dewaele, G.F. Froment, TAP study of the mechanism and kinetics of the adsorption and combustion of methane on Ni/Al_2O_3 and NiO/Al_2O_3, J. Catal. 184 (1999) 499–513.
[70] G. Xu, K. Shi, Y. Gao, H. Xu, Y. Wei, Studies of reforming natural gas with carbon dioxide to produce synthesis gas: the role of CeO_2 and MgO promoters, J. Mol. Catal. A: Chem. 147 (1999) 47–54.
[71] Y. Cesteros, P. Salagre, F. Medina, J.E. Sueiras, Effect of the alumina phase and its modification on Ni/Al_2O_3 catalysts for the hydrodechlorination of 1,2,4-trichlorobenzene, Appl. Catal. B: Environ. 22 (1999) 135–147.
[72] J.T. Miller, B.L. Meyers, F.S. Modica, G.S. Lane, M. Vaarkamp, D.C. Koningsberger, Hydrogen temperature programmed-programmed desorption (H_2 TPD) of supported platinum catalysts, J. Catal. 143 (1993) 395–408.
[73] R.W. Wunder, J.W. Cobes, J. Phillips, Microcalorimetric study of the absorption of hydrogen by palladium powders and carbon-supported palladium particles, Langmuir 9 (1993) 984–992.
[74] P.A. Sermon, G.C. Bond, Hydrogen spillover, Catal. Rev. 8 (1973) 211–239.
[75] A.D. Lueking, R.T. Yang, Hydrogen spillover to enhance hydrogen storage—study of the effect of carbon physicochemical properties, Appl. Catal. A: Gen. 265 (2004) 259–268.
[76] P. Baeza, M.S. Ureta-Zanartu, N. Escalona, J. Ojeda, F.J. Gil-Llambias, B. Delmon, Migration of surface species on supports: a proof of their role on the synergism between CoS_x or NiS_x and MoS_2 in HDS, Appl. Catal. A: Gen. 274 (2004) 303–309.
[77] N. Ansari, R. Balasubramaniam, Determination of hydrogen diffusivity in nickel by subsurface microhardness profiling, Mater. Sci. Eng. A 293 (2000) 292–295.
[78] D.S. Dos Santos, H-diffusivity and solubility in crystalline Pd–Ni alloys, Defect Diffus. Forum 203-202 (2002) 219–224.
[79] F. Faccin, F.F. Guedes, E.V. Benvenutti, C.C. Moro, FTIR study of the metal-support interactions and hydrogen spillover on Pd/TiO_2 and Ni/TiO_2, Eclet. Quim. 27 (2002) 93–102.
[80] P.C.H. Mitchell, A.J. Ramirez-Cuesta, S.F. Parker, J. Tomkinson, D. Thompsett, Hydrogen spillover on carbon-supported metal catalysts studied by inelastic neutron scattering. Surface vibrational states and hydrogen riding modes, J. Phys. Chem. B 107 (2003) 6838–6845.
[81] S.J. Teichner, Recent studies in hydrogen and oxygen spillover and their impact on catalysis, Appl. Catal. 62 (1990) 1–10.
[82] B. Coq, G. Ferrat, F. Figueras, Conversion of chlorobenzene over palladium and rhodium catalysts of widely varying dispersion, J. Catal. 101 (1986) 434–445.
[83] V. Simagina, V. Likholobov, G. Bergeret, M.T. Gimenez, A. Renouprez, Catalytic hydrodechlorination of hexachlorobenzene on carbon supported Pd-Ni bimetallic catalysts, Appl. Catal. B: Environ. 40 (2003) 293–304.
[84] M.A. Keane, G. Pina, G. Tavoularis, The catalytic hydrodechlorination of mono-, di- and trichlorobenzenes over supported nickel, Appl. Catal. B: Environ. 48 (2004) 275–286.
[85] A.R. Suzdorf, S.V. Morozov, N.N. Anshits, S.I. Tsiganova, A.G. Anshits, Gas phase hydrodechlorination of chlorinated aromatic compounds on nickel catalysts, Catal. Lett. 29 (1994) 49–55.
[86] C. Menini, G. Tavoularis, C. Park, M.A. Keane, Catalytic hydrodehalogenation as a detoxification methodology, Catal. Today 62 (2000) 355–366.
[87] B.F. Hagh, D. Allen, Catalytic hydroprocessing of chlorinated benzenes, Chem. Eng. Sci. 45 (1990) 2695–2701.
[88] Y. Liu, W. Wu, Y. Guan, P. Ying, C. Li, FT-IR spectroscopic study of the oxidation of chlorobenzene over Mn-based catalyst, Langmuir 18 (2002) 6229–6232.
[89] L.D. Asnin, A.A. Fedorov, Adsorption of chlorobenzene on γ-Al_2O_3 obtained by calcination of boehmite at various temperatures, Russ. J. Appl. Chem. 76 (2003) 719–722.